Edge-Soliton-Mediated Vortex-Core Reversal Dynamics

Ki-Suk Lee, Myoung-Woo Yoo, Youn-Seok Choi, and Sang-Koog Kim*

National Creative Research Initiative Center for Spin Dynamics & Spin-Wave Devices, Nanospinics Laboratory, Research Institute of Advanced Materials, Department of Materials Science and Engineering, Seoul National University, Seoul 151-744, Republic of Korea

(Received 29 November 2010; published 4 April 2011)

We report an additional reversal mechanism of magnetic vortex cores in nanodot elements driven by currents flowing perpendicular to the sample plane, occurring via dynamic transformations between two coupled edge solitons and bulk vortex solitons. This mechanism differs completely from the well-known switching process mediated by the creation and annihilation of vortex-antivortex pairs in terms of the associated topological solitons, energies, and spin-wave emissions. Strongly localized out-of-plane gyrotropic fields induced by the fast motion of the coupled edge solitons enable a magnetization dip that plays a crucial role in the formation of the reversed core magnetization. This work provides a deeper physical insight into the dynamic transformations of magnetic topological solitons in nanoelements.

DOI: 10.1103/PhysRevLett.106.147201 PACS numbers: 75.78.Jp, 75.78.Cd, 75.78.Fg

Nontrivial inhomogeneous magnetization configurations in the restricted geometries of micrometer-size (or smaller) magnetic elements play crucial roles in the magnetization dynamics occurring on scales of a few tens of picoseconds [1–5]. Such dynamics have attracted growing interest for their potential applications to future data storage [6–8] and processing devices [9,10]. For example, domain wall motion can be described in terms of the dynamics of various types of magnetic topological solitons, i.e., transverse, vortex, and antivortex walls, via the sequential processes of the creation, propagation, and annihilation of them [3,4] in the Walker breakdown regime in magnetic nanostrips or simple motions of single solitons without any transformation of their internal structures [5]. Also, a single magnetic vortex in nanodots can be transformed into a new vortex with its core orientation opposite to the original core orientation via the serial processes of the creation and subsequent annihilation of vortex-antivortex (VAV) pairs, with the help of vortex-core (VC) gyration motions [11–17].

Furthermore, it has been reported that VC reversals can take place, possibly avoiding VC motions, under a specific condition of an intended immobile VC [18], by application of strong pulse fields perpendicular to the sample plane [19], or through a thermal excitation [20]. Regardless of the particular conditions and types of driving forces, the common reversal mechanism found thus far is the dynamic process of VAV-pair creation followed immediately by the annihilation of the newly created antivortex and the original vortex inside the nanoelements. Such core reversals are always accompanied by an exchange energy explosion and subsequent spin-wave emissions phenomena.

In this Letter, we report a novel VC reversal mechanism driven by currents flowing perpendicular to the sample plane, which occurs through the creation of two coupled edge solitons of half-integer winding number topological charge, not followed by exchange energy explosion and spin-wave emission phenomena. The physical origin of the edge-soliton-mediated VC reversals are also addressed.

Our approach in this study was to use micromagnetic numerical simulation, owing to its sufficient spatial and temporal resolutions and reliable resulting outputs for the given model's dimensional scales. We employed a model system constituting free-standing permalloy (Py, $Ni_{80}Fe_{20}$) [21] thin-film disks of $2R = 200$ nm diameter and $L = 7$ nm thickness [Fig. 1(a)]. For vortex excitations up to its core switching, we used out-of-plane dc currents applied in the $+z$ direction (designated as $i_p = +1$) and a perpendicular polarizer of the spin-polarization direction $\hat{\mathbf{m}}_P = S_{\mathrm{pol}}\hat{\mathbf{z}}$ with $S_{\mathrm{pol}} = -1$. Such current flows produce two different effects: spin transfer torque (STT), and in-plane circumferential Oersted field (OH) around the given current pass [22,23]. We took into account both effects in all the simulations. The OOMMF code (version 1.2a4) used [24] incorporates the Landau-Lifshitz-Gilbert equation

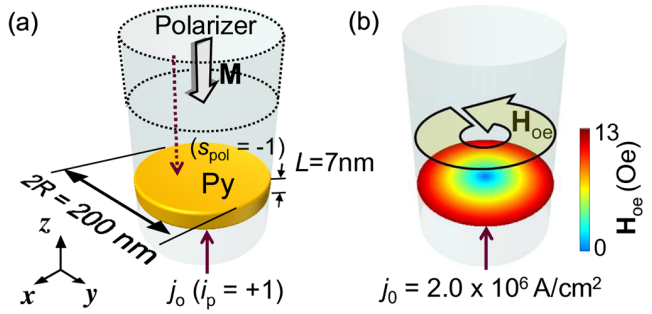

FIG. 1 (color online). Schematic illustration of model system. (a) Free-standing Py disk of indicated dimensions. (b) Spatial distribution of strength of OHs induced by current flow of the indicated density j_0. The wide arrow and color-coded bar indicate the in-plane rotation sense (here, CCW for $i_p = +1$) and the strength, respectively.

[25] and an additional STT term [26]: $d\mathbf{M}/dt = -\gamma'\mathbf{M} \times \mathbf{H}_{\text{eff}} + \alpha/|\mathbf{M}|[\mathbf{M} \times (\mathbf{M} \times \mathbf{H}_{\text{eff}})] + \mathbf{T}_{\text{STT}}$, where $\gamma' = \gamma/(1+\alpha^2)$ with the phenomenological damping constant α, the gyromagnetic ratio γ, and the effective field $\mathbf{H}_{\text{eff}}$. The STT is given by $\mathbf{T}_{\text{STT}} = (a_{\text{STT}}/|\mathbf{M}|)\mathbf{M} \times (\mathbf{M} \times \hat{\mathbf{m}}_P)$ with $a_{\text{STT}} = \frac{1}{2\pi} h\gamma P j_0/(\mu_0 2eM_s L)$, where h is the Planck's constant, j_0 the current density, μ_0 the vacuum permeability, e the electron charge, M_s the saturation magnetization, and the degree of spin polarization, here $P = 0.7$ [14]. We assumed that in the current-perpendicular-to-plane geometry, currents flow uniformly through the entire Py disk [see Fig. 1(b)]. The initial ground state [27] of a magnetic vortex is the upward core magnetization, corresponding to the polarization $p = +1$ and the counterclockwise (CCW) in-plane curling magnetization, chirality $C = +1$. The other parameters applied were as follows: $\alpha = 0.01$, $\gamma = 2.21 \times 10^5$ m/A s, and unit cell size, $2 \times 2 \times 7$ nm^3.

Figure 2 shows the results of the numerical simulations. According to the current density j_0, the observed dynamic behaviors were very distinct. We observed stationary VC gyrations [28–30] with the CCW rotation sense in a range of $1.15 \times 10^6 \leq j_0$ (A/cm^2) $< 1.6 \times 10^6$, notably, persistently rotating motions of two coupled edge solitons within the range of $1.6 \times 10^6 \leq j_0$ (A/cm^2) $< 2.4 \times 10^6$, and VC reversals in a higher current density regime, here $2.4 \times 10^6 \leq j_0$ (A/cm^2) $< 1.8 \times 10^8$. In the dynamic regime of the motion of the coupled edge solitons, hitherto unknown, the initial VC gyrates with a continuously increasing orbit radius, and when it reaches the disk boundary, it is then transformed into a quasiuniform magnetization structure in a C-like deformation state. This transient process results in the two coupled edge solitons that rotate constantly in the same CCW sense as that of the initial upward core, as evidenced by the corresponding solitons' trajectory at $j_0 = 2.0 \times 10^6$ A/cm^2 (Fig. 2, middle). In the range of $2.4 \times 10^6 \leq j_0$ (A/cm^2) $< 1.5 \times 10^8$, however, the persistent rotation motion of the edge-soliton pair observed in the range of $1.6 \times 10^6 \leq j_0$ (A/cm^2) $< 2.4 \times 10^6$ is no longer stable, but this pair is transformed into the downward VC, $p = -1$ (Fig. 2, right). Once the reversed core ($p = -1$) is formed, it experiences a damped gyration with decreasing orbit radius in the clockwise (CW) rotation sense. Finally, the VC reversal is completed through the creation and annihilation of the edge-soliton pair, rather than the well-known VAV-pair-mediated mechanism reported in Refs. [11–17].

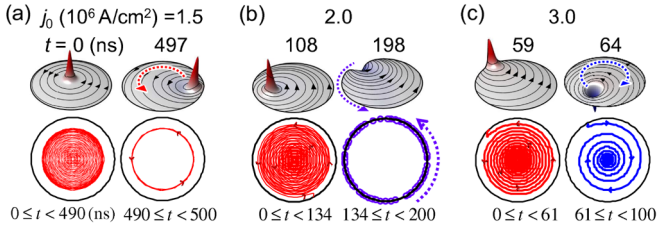

FIG. 2 (color online). Representative distinct vortex excitations driven by out-of-plane dc currents in different regions of j_0. For each region we chose $j_0 = 1.5$ (a), 2.0 (b), and 3.0×10^6 A/cm^2 (c), respectively. Top of each j_0: snapshot perspective images of temporal evolution of vortex dynamics. The height of the surface indicates the out-of-plane components of the local magnetizations, and the streamlines with arrows indicate the in-plane components. Bottom of each: trajectories of in-plane motions of upward (red) VC and its reversed downward (blue) core, or coupled edge solitons (purple).

In order to elucidate the edge-soliton-mediated reversal dynamics, we studied the details of the transformation subprocesses from the standpoint of topological solitons, as shown in Fig. 3. The edge-soliton-mediated mechanism consists of three distinct processes: (1) annihilation of the original single vortex, once it reaches the disk boundary via core gyration, (2) formation of two coupled edge solitons, and (3) creation of a reversed core vortex through fusion of the coupled edge solitons. The transition from process 1 to process 2 is spontaneous, as evidenced by no energy barrier to the annihilation of the initial VC when it reaches the edge boundary (see comparison of energy plots in Fig. 3). By contrast, the transition from process 2 to process 3 is not spontaneous, as evidenced by the emergence of the

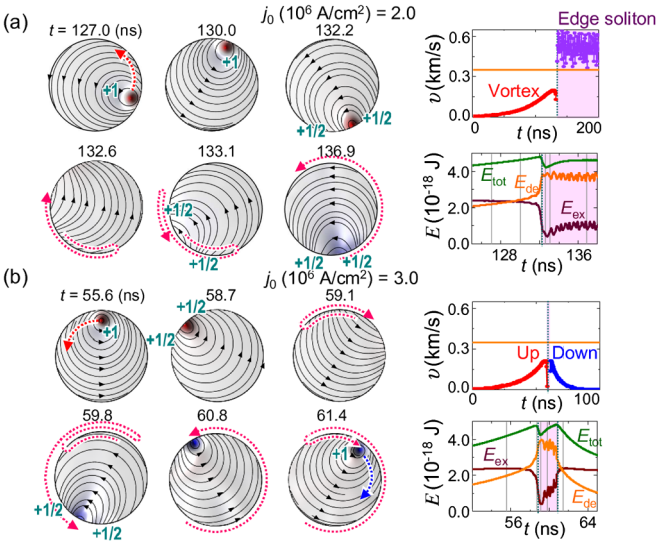

FIG. 3 (color online). Comparison of two different dynamic behaviors associated with two coupled edge solitons: (a) in-plane persistent rotation of two edge solitons at disk boundary and (b) transformation to VC of reversed orientation. The color coding indicates the out-of-plane components of the local magnetizations, while the streamlines with arrows indicate the in-plane components. The dotted red arrows represent the directions of the motion of the coupled edge solitons. The right column shows the exchange (E_{ex}), demagnetization (E_{de}) energies and their sum (E_{tot}), and velocity (v) variations, where the vertical lines are drawn at the indicated times shown in the corresponding snapshot images (left). The orange horizontal lines represent the value of $v = 350$ m/s.

stationary motion of the coupled edge solitons along the disk edge within a broad range of 1.6×10^6 A/cm$^2 \leq j_0 < 2.4 \times 10^6$ A/cm^2, and by the fact that the coupled edge solitons in their persistent motion are transformed into the vortex of the reversed core only with further increase in j_0. This reveals that the edge-soliton pair must overcome an exchange energy barrier for the formation of the reversed VC inside the disk. In this case, an exchange energy explosion and resultant spin-wave emissions typically found in the VAV-mediated core reversals disappear and rather the demagnetization energy of the two edge solitons rapidly decreases when the reversed VC starts to form inside the disk.

From the two-dimensional (2D) topological perspective [2,31], the dynamic transformation from a single vortex to a coupled edge-soliton state (and vice versa) occurs while conserving the total winding number (n) topological charge of the solitons involved in the process [2]. The initial single vortex denoted as a bulk ($n = +1$) soliton decomposes into two coupled edge ($n = +1/2$) solitons, holding the total winding number, $n = +1$. However, another topological charge, the Skyrmion number [32,33] defined as $q = np/2$ decays from the up core ($q = +1/2$) into two edge solitons ($q = 0$). Subsequently, a reversed down core ($q = -1/2$) is created from the fusion of the two $q = 0$ edge solitons. In the well-known VAV-mediated reversals, the total $+1$ (or -1) Skyrmion charge of the original upward (or downward) VC [$q = +1/2$ (or $-1/2$)] and the newly created downward (or upward) antivortex [$q = +1/2$ (or $-1/2$)] decays to 0 via their annihilation, accompanied by spin-wave emissions [12,33,34]. In contrast, in the edge-soliton mediated process the exchange energy of the $q = +1/2$ Skyrmion, rather than drastically dissipating through spin-wave emissions as in the VAV-mediated reversals, converts to the magnetostatic energy of the edge solitons (see Fig. 3, plot of energies) in which process the magnetostatic energy is converted back to the exchange energy of the reversed VC. This is because the 0 Skyrmion number of the edge-soliton pair has a strong magnetostatic energy due to magnetic free poles at the disk edge boundary. It is worth noting that the edge-soliton-mediated core reversals occur because the original VC reaches the dot boundary prior to attaining the critical velocity required for the VAV-pair-mediated core reversals inside the disk. As revealed by the velocities of the original VCs versus time (Fig. 3, right column), this mechanism does not require the critical velocity for core magnetization reversals.

Next, to elucidate the exact origin of the transformation of a persistently rotating edge-soliton pair into a reversed VC, we introduce the out-of-plane gyrotropic field h_z that plays a crucial role, as the physical origin of VAV-pair-mediated reversals, in the formation of a dip where the magnetization is strongly localized and opposite to the original core magnetization [15]. The h_z is expressed in the form $-1/(\gamma M_s^2)[\mathbf{M} \times (d\mathbf{M}/dt)]_z$, as derived from the time-derivative term of the LLG equation [35,36]. Then, from the acquired numerical data obtained from further micromagnetic simulations [37], we directly calculated both the local h_z (right) and the out-of-plane magnetization m_z (left) distributions for three representative values of j_0, as shown in Fig. 4(a). As can be seen, the m_z and h_z are strongly concentrated locally between the two edge solitons. The maximum h_z value, indicated by the red spot, is found there [Fig. 4(a), right, bottom]. Such concentrations grow higher with larger current densities, and correspondingly, the two edge solitons move closer together, inducing largely concentrated in-plane curling magnetization distortion between them, and then a highly concentrated h_z.

We also plotted the maxima of the h_z and m_z values averaged over the steady motion of the edge-soliton pair as a function of j_0 up to the VC reversal. In this case, the velocity of the edge solitons' motion reaches a value, 531 ± 153 m/s, higher than the critical velocity (about 330 ± 37 m/s for Py) required for VAV-mediated core reversals [15,16]. As seen in Fig. 4(b), as j_0 increases, the negative maxima of the h_z and m_z grow with the velocity of the coupled edge-soliton motion. This is owed to the fact that the $d\mathbf{M}/dt$ in the h_z equation can be expressed as $-(\boldsymbol{v} \cdot \nabla)\mathbf{M}$ [15,35] for the motion of the edge-soliton pair with velocity $\boldsymbol{v}$; therefore, the h_z is proportional to v and the distortion of the in-plane

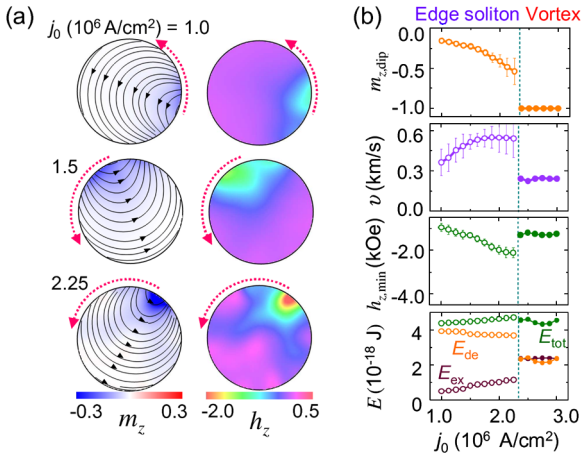

FIG. 4 (color online). (a) Spatial distributions of magnetization deformation m_z (left) and normal component of associated out-of-plane gyrotropic field h_z (right), for indicated j_0 values, as indicated by corresponding color codes. The streamlines with arrows indicate the in-plane local magnetizations. (b) Plots of magnetization dip $m_{z,\mathrm{dip}} = M_{z,\mathrm{dip}}/M_s$ and minima of local h_z as functions of j_0 along with the velocity of motion of coupled edge solitons and associated energy variation. The vertical dotted line indicates the boundary above which value VC reversals occur through the two coupled edge solitons. Above j_0 marked by the dotted vertical line, each value was estimated at the time when the reversed VC starts to gyrate with the characteristic damping motion.

magnetization, as shown in Fig. 4(a). With further increases of j_0, beyond the critical value (here $j_{0,\mathrm{cri}} = 2.4 \times 10^6$ A/cm^2), the strength of $h_{z,\mathrm{min}}$ itself reaches a certain critical value ($h_{z,\mathrm{cri}} = -2.1 \pm 0.2$ kOe), allowing for a magnetization dip in the direction opposite to the original core magnetization, which dip is necessary for the formation of the reversed core orientation, as reported in our earlier studies [15,16,36]. In the range of $1.6 \times 10^6 \leq j_0(\mathrm{A/cm^2}) < 2.4 \times 10^6$, the strength of h_z, however, is not sufficient to create, from the dip, a new vortex with its reversed core orientation, and thus, the rotating motion of the edge-soliton pair is maintained.

Finally, we note that the STT and in-plane OH do not directly cause the magnetization dip around the edge solitons. Rather, the STT accelerates the rotating motion of the edge solitons, inducing a strongly localized h_z that results in the formation of the magnetization dip, thereby the creation of the reversed VC. Nonetheless, the OH plays a major role in the determination of the in-plane curling magnetization direction of the C-like configuration, as found from further simulations excluding the OH effect. We also note that the shape anisotropy of an elliptical disk can affect the dynamic motion of edge-soliton pairs, but does not contribute significantly to the switching mechanism, as revealed from additional simulations.

To conclude, we discovered an additional reversal mechanism of magnetic VCs in nanodisks driven by out-of-plane currents. This reversal mechanism occurs through dynamic transformations between two coupled half-integer edge solitons and integer bulk vortex solitons. The mechanism differs completely from the well-known VAV reversal process in the types of the associated topological solitons, energies, and spin-wave emissions. This work provides a deeper insight into fundamentals of the dynamic transformations of magnetic solitons of different topological charges in nanoelements.

This work was supported by the Basic Science Research Program through the National Research Foundation of Korea (NRF) funded by the Ministry of Education, Science and Technology (Grant No. 20100000706).

*To whom all correspondence should be addressed. sangkoog@snu.ac.kr

[1] V. G. Bar'yahhtar *et al.*, *Dynamics of Topological Magnetic Solitons* (Springer-Verlag, Berlin, 1994); A. Hubert and R. Schäfer, *Magnetic Domains* (Springer-Verlag, Berlin, New York, Heidelberg, 1998).
[2] O. Tchernyshyov and G. W. Chern, Phys. Rev. Lett. **95**, 197204 (2005).
[3] J.-Y. Lee *et al.*, Phys. Rev. B **76**, 184408 (2007); K. Y. Guslienko, J.-Y. Lee, and S.-K. Kim, IEEE Trans. Magn. **44**, 3079 (2008).
[4] D. J. Clarke *et al.*, Phys. Rev. B **78**, 134412 (2008).
[5] R. Wieser *et al.*, Phys. Rev. B **82**, 144430 (2010), M. Yan *et al.*, Phys. Rev. Lett. **104**, 057201 (2010).
[6] S. S. P. Parkin, M. Hayashi, L. Thomas, Science **320**, 190 (2008).
[7] R. P. Cowburn, Nature Mater. **6**, 255 (2007); J. Thomas, Nature Nanotech. **2**, 206 (2007).
[8] S.-K. Kim *et al.*, Appl. Phys. Lett. **92**, 022509 (2008); S.-K. Kim *et al.*, IEEE Trans. Magn. **44**, 3071 (2008).
[9] D. A. Allwood *et al.*, Science **309**, 1688 (2005).
[10] Q. Mistral *et al.*, Phys. Rev. Lett. **100**, 257201 (2008); V. S. Pribiag *et al.*, Phys. Rev. B **80**, 180411 (2009); A. Ruotolo *et al.*, Nature Nanotech. **4**, 528 (2009).
[11] B. Van Waeyenberge *et al.*, Nature (London) **444**, 461 (2006); A. Vansteenkiste *et al.*, Nature Phys. **5**, 332 (2009).
[12] S. Choi *et al.*, Phys. Rev. Lett. **98**, 087205 (2007); K.-S Lee *et al.*, Phys. Rev. B **76**, 174410 (2007).
[13] R. Hertel *et al.*, Phys. Rev. Lett. **98**, 117201 (2007).
[14] K. Yamada *et al.*, Nature Mater. **6**, 270 (2007); S.-K. Kim *et al.*, Appl. Phys. Lett. **91**, 082506 (2007).
[15] K. Y. Guslienko, K.-S. Lee, and S.-K. Kim, Phys. Rev. Lett. **100**, 027203 (2008).
[16] K.-S. Lee *et al.*, Phys. Rev. Lett. **101**, 267206 (2008).
[17] D. D. Sheka *et al.*, Appl. Phys. Lett. **91**, 082509 (2007).
[18] V. P. Kravchuk *et al.*, Phys. Rev. B **80**, 100405 (2009).
[19] A. Killinger, R. Hollinger, and U. Krey, J. Magn. Magn. Mater. **272–276**, 724 (2004).
[20] R. Wieser, K. D. Usadel, and U. Nowak, Phys. Rev. B **74**, 094410 (2006).
[21] The material parameters for Py in this simulation were the magnetization saturation $M_s = 8.6 \times 10^5$ A/m, the exchange stiffness $A_{\mathrm{ex}} = 1.3 \times 10^{-11}$ J/m, and a zero magnetocrystalline anisotropy constant.
[22] Y.-S. Choi *et al.*, Appl. Phys. Lett. **93**, 182508 (2008).
[23] Y.-S. Choi, K.-S. Lee, and S.-K. Kim, Phys. Rev. B **79**, 184424 (2009).
[24] See http://math.nist.gov/oommf.
[25] L. D. Landau and E. M. Lifshitz, Phys. Z. Sowjetunion **8**, 153 (1935); T. L. Gilbert, Phys. Rev. **100**, 1243 (1955).
[26] J. C. Slonczewski, J. Magn. Magn. Mater. **159**, L1 (1996); L. Berger, Phys. Rev. B **54**, 9353 (1996).
[27] To excite the vortex gyration mode by out-of-plane dc currents, the initial VC was displaced 2 nm away from the center poistion in the $-x$ direction.
[28] Y.-S. Choi *et al.*, Appl. Phys. Lett. **96**, 072507 (2010).
[29] B. A. Ivanov and C. E. Zaspel Phys. Rev. Lett. **99**, 247208 (2007); A. V. Khvalkovskiy *et al.*, Phys. Rev. B **80**, 140401 (2009).
[30] A. Dussaux *et al.*, Nature Commun. doi:10.1038/ncomms1006 (2010).
[31] N. D. Mermin, Rev. Mod. Phys. **51**, 591 (1979).
[32] T. H. R. Skyrme, Proc. R. Soc. London A **262**, 237 (1961).
[33] O. A. Tretiakov and O. Tchernyshyov, Phys. Rev. B **75**, 012408 (2007).
[34] K.-S. Lee, S. Choi, and S.-K. Kim, Appl. Phys. Lett. **87**, 192502 (2005); R. Hertel and C. M. Schneider, Phys. Rev. Lett. **97**, 177202 (2006).
[35] A. A. Thiele, Phys. Rev. Lett. **30**, 230 (1973).
[36] M.-Y Yoo *et al.*, Phys. Rev. B **82**, 174437 (2010).
[37] To reduce the computational time, we intended to form two edge solitons by application of a 400 Oe static external field in the $+y$ direction. This field would allow for C-state magnetization deformation.